

UNCLASSIFIED

AD 295 721

*Reproduced
by the*

**ARMED SERVICES TECHNICAL INFORMATION AGENCY
ARLINGTON HALL STATION
ARLINGTON 12, VIRGINIA**



UNCLASSIFIED

NOTICE: When government or other drawings, specifications or other data are used for any purpose other than in connection with a definitely related government procurement operation, the U. S. Government thereby incurs no responsibility, nor any obligation whatsoever; and the fact that the Government may have formulated, furnished, or in any way supplied the said drawings, specifications, or other data is not to be regarded by implication or otherwise as in any manner licensing the holder or any other person or corporation, or conveying any rights or permission to manufacture, use or sell any patented invention that may in any way be related thereto.

63-2-3

TECHNICAL INFORMATION SERIES

CATALOGED BY ASTIA
AD No. 295721

R63SD5

MAGNETOHYDRODYNAMIC PROPULSION *

A. SHERMAN

SPACE SCIENCES LABORATORY

GENERAL  ELECTRIC

MISSILE AND SPACE DIVISION

295 721

* THIS WORK WAS SPONSORED BY THE AIR FORCE OFFICE OF SCIENTIFIC RESEARCH,
OFFICE OF AEROSPACE RESEARCH, UNDER CONTRACT AF49(638)-914

SPACE SCIENCES LABORATORY
AEROPHYSICS SECTION

MAGNETOHYDRODYNAMIC PROPULSION*

by

A. Sherman

* This work was sponsored by the Air Force Office of Scientific Research, Office of Aerospace Research, under Contract AF 49(638)-914.

R63SD5
January, 1963

MISSILE AND SPACE DIVISION

GENERAL  ELECTRIC

CONTENTS

PAGE

13.1	Introduction	1
13.2	Crossed Field Devices	4
13.3	The Hall Current Accelerator	12
13.4	Pulsed Accelerators Employing Electrodes	16
13.5	Electrodeless Accelerators	21

FOREWORD

This report has been written as Chapter 13 of a forthcoming book, *Engineering Magnetohydrodynamics*. References to other chapters refer to chapters in that book.

13.1 INTRODUCTION

To complete this presentation of Engineering Magnetohydrodynamics, two areas of application, namely; Magnetohydrodynamic Propulsion and Power Generation, will be treated. The present chapter will deal with the former. Due to the considerable amount of current work in this area it will not be possible to cover the subject completely. An attempt will be made, rather, to describe the physical operation of a number of different types of propulsion units, to identify their unusual characteristics, and to define desirable operating modes.

Magnetohydrodynamic accelerators are only one of several types of electrical propulsion devices being proposed for use in space flight. Although the application of electrical propulsion devices to space propulsion has been studied extensively⁽¹⁾ it may be in order to discuss this question briefly. Up to the present time all space propulsion has been accomplished with chemical rockets. They give thrust to weight ratios greater than unity and are in a high state of development. Their limitation is that they can give, at most, specific impulses (rocket exhaust velocity/acceleration due to gravity at earth's surface) in the order of 400 seconds. This limitation is due to the fact that there is a practical limit to the energy available from a chemical reaction so that the total enthalpy available for conversion into exhaust kinetic energy is limited. If, however, the molecular weight of the exhaust gases are lowered the specific impulse can be raised. This is the principle employed in the nuclear rocket concept where gaseous Hydrogen is used as the propellant. In other words, for a given initial total temperature the limiting exhaust velocity (exhaust temperature zero) is given by

$$u_{\text{limit}} = \sqrt{2 c_p T_o / M} \quad (13.1)$$

where c_p now is the molar specific heat which does not vary appreciably from one gas to another and where M is the molecular weight. Thus, the specific impulse varies inversely as the square root of the molecular weight, and Hydrogen is an obvious choice. Since 3000°K is the upper limit of T_o in a nuclear rocket utilizing a heat exchanger, the specific impulse will be limited to less than 1000 seconds. When the limitation on total temperature is removed, as in an electrical rocket, then there is no limit to the specific impulse that may be achieved. There is a limit, however, to the specific impulse that may be achieved efficiently. The question of efficiency is an essential one since the electrical rocket uses energy provided by some power supply, and if it does not use it efficiently the power supply becomes excessively heavy. Another essential feature of the

electrical propulsion system is that it has a thrust to weight ratio much less than unity so that it must be launched, or placed into orbit, by a chemical or nuclear rocket.

The desirability of a high value of specific impulse for space flight can be established by a simple argument. Consider a space craft moving at a constant velocity (\sim exhaust velocity) between two points in space. Now a mission can generally be defined in terms of the thrust on the vehicle times the length of time it is applied. In other words the total impulse is

$$I \equiv \int_0^{t_f} T dt = \int_0^{t_f} \dot{m} v dt = m v \quad (13.2)$$

where T is thrust, \dot{m} is propellant flow rate, and m is total propellant mass expended during the mission*. It is clear that the higher the exhaust velocity the less propellant mass used. Where the total mass of propellant is limited, as for example in extremely long missions (\sim 1 year), the above considerations become critical.

Actually from the above simple argument one would suppose that the maximum possible specific impulse would be the most desirable. This is not the case. In fact there is an optimum specific impulse for each vehicle and mission. This can be illustrated by considering the weight of the electrical power supply needed to operate the electrical rocket. First, define the mass advantage γ of the electrical system over the chemical system as

$$m_{\text{elec}} + m_{\text{ps}} \equiv \gamma m_{\text{chem}} \quad (13.3)$$

where m_{ps} is the mass of the electrical power supply, m_{chem} is the total mass of the chemical propellant, m_{elec} is the total mass of the electrical rocket propellant, and $\gamma < 1$. If the same mission is to be performed by both devices then

$$I = m_{\text{chem}} v_{\text{chem}} = m_{\text{elec}} v_{\text{elec}} \quad (13.4)$$

or using (13.3)

$$\frac{m_{\text{ps}}}{m_{\text{elec}}} = \gamma \frac{v_{\text{elec}}}{v_{\text{chem}}} - 1 \quad (13.5)$$

*Equation (13.2) illustrates the alternate definition of specific impulse as $I_{\text{sp}} = T/\dot{m}$, where its units are those of velocity. If, however, the \dot{m} is given in terms of weight flow rather than mass flow then I_{sp} is again in units of time. For the purposes of the present chapter I_{sp} will be defined as v/g as noted earlier.

If the quantity α , the specific weight of the power supply, is defined as the ratio of m_{ps} to power supply power level P then

$$\alpha = \frac{m_{ps}}{P} \quad (13.6)$$

Assuming an electrical rocket with an efficiency η we can write $\eta P = \frac{1}{2} \dot{m}_{elec} v_{elec}^2$ so that

$$\frac{m_{ps}}{m_{elec}} = \frac{\frac{1}{2} \alpha \dot{m}_{elec} v_{elec}^2}{\eta \dot{m}_{elec}} = \frac{\alpha v_{elec}^2}{2 t_f \eta} \quad (13.7)$$

Substituting this into equation (13.5) yields an expression for γ .

$$\gamma = \frac{v_{chem}}{v_{elec}} + \frac{1}{2} \frac{\alpha}{t_f \eta} v_{elec} v_{chem} \quad (13.8)$$

Clearly there is some value of v_{elec} (or specific impulse) which makes γ a minimum. Taking $d\gamma/dv_{elec} = 0$ the above yields this optimum.

$$(v_{elec})_{opt} = \sqrt{\frac{2 t_f \eta}{\alpha}} \quad (13.9)$$

According to this simple relation the longer the mission the higher the optimum specific impulse. Also, the heavier the power supply the smaller the optimum value, so that one can anticipate that if the power supply is too heavy the optimum I_{sp} will become so low that a chemical rocket can do the job with less total weight. Also note that the electrical rocket inefficiency can be absorbed directly in a larger power supply specific weight. Assuming an α of 30#m/kw equation (13.9) shows that $(I_{sp})_{opt} \sim 4000$ seconds for lunar missions (100 days), and $\sim 12,000$ seconds for interplanetary missions (1000 days). These values are surprisingly close to the results of more precise calculations^(2,3). Also, equation (13.8) shows that $\gamma \sim 0.20$ for the former and ~ 0.07 for the latter, illustrating the anticipated superiority of the electrical propulsion system compared to the chemical system as far as payload mass is concerned. Finally, it can be seen that using equation (13.9) then equation (13.7) yields the interesting conclusion that the optimum condition for a mission is that the power supply and propellant masses be equal.

As a result of the above discussion it should now be clear that in order for an electrical propulsion system to be useful for space missions it must have a light weight power supply (small α), and it must have an electrical rocket capable of efficient operation at impulse values in the range of 2000 - 20,000

seconds. It is because the Magnetohydrodynamic propulsion unit offers the potential for efficient operation in this specific impulse range that there is much current interest in it^(4, 5).

In the remainder of this chapter a number of specific devices will be discussed in detail. No attempt will be made to classify them in any precise way. The first section will deal with crossed field devices operating at sufficiently high pressures that the Hall effect is of secondary importance. These will generally be high thrust per unit area machines. Following this, related devices operating at lower pressures will be discussed, in which the Hall currents dominate. The subject of the electrodeless machine will be taken up next since in some of its manifestations it is a quasisteady device. Concluding the chapter will be discussions of pulsed accelerators with electrodes. Compared to the crossed field device these others are all essentially low thrust per unit area machines. Compared to the Ion rocket however they can all be considered as having a high thrust per unit area.

13.2 CROSSED FIELD ACCELERATORS

As pointed out earlier the specific impulse of an electrical rocket can be made to exceed that of a chemical rocket by the simple expedient of raising the propellants total temperature prior to expansion through the nozzle. If the question of efficiency is considered, however, it is quickly seen that such a process cannot go on indefinitely. As a gas is heated to higher and higher temperatures it dissociates and ionizes and the energy invested in these modes will generally be lost in the subsequent frozen expansion, causing the entire process to be inefficient. In order to avoid this difficulty as higher specific impulses are sought, it would seem advisable to maintain a more modest static temperature and add additional energy directly into kinetic energy via the Lorentz force. This approach is common to all of the devices to be considered in the present chapter. In the present section an accelerator in which mutually perpendicular applied electric and magnetic fields create the Lorentz force will be treated. As could have been anticipated the principle questions will concern specific impulse and efficiency.

Since crossed field devices have been described several times (i.e. chapters 10 and 11) there is no need to repeat these descriptions again here. It should suffice to point out that for such a device to operate as an accelerator the vector product of the current and magnetic field should lie in the flow direction. Basically, the device will operate with a relatively high pressure compressible reacting

plasma in supersonic flow. The induced magnetic field will be negligible, but the Hall effect may not, in which case segmented electrodes may be used.

Before discussing some of the theoretical and experimental studies that have been carried out it would be of value to consider the questions of specific impulse and efficiency in the broad sense. In general, the accelerating capability of any crossed field device will depend on the magnetic interaction parameter based

on its length ($Q = \frac{\sigma_0 B_0^2 L}{\rho_0 u_0}$). It is obvious, then, that one way to obtain a very high I_{sp} in a short distance is to reduce the gas density. Doing this, however, will require the use of segmented electrodes to avoid the Hall current flow. Generally speaking modest increases in I_{sp} can be achieved without the need to consider the Hall effect, or use segmented electrodes, but it will have to be taken into account for higher I_{sp} values.

In regard to efficiency the important problem is the losses. They may be enumerated as follows:

1. Thermal energy remaining in plasma stream at accelerator exit.
2. Ionization and dissociation energy remaining in stream at accelerator exit.
3. Heat and momentum transferred from main stream into accelerator walls.

If regenerative cooling is used some of item 3 may be recovered and will not properly count as an energy loss. It will, in any event, degrade the performance of the crossed field accelerator (i.e. require additional length to achieve some desired I_{sp}). End effects which can also degrade the performance will be neglected here. They are considered in some detail in the next chapter on power generation.

As was seen in Chapter 11 a large number of solutions are possible to the quasi-one dimensional equations, many of which can be utilized for crossed field accelerators. Recalling the requirement to minimize frozen flow losses a logical choice would at least have $t = \text{constant}$. Following this reasoning Wood⁽⁶⁾ and Kerrebrock⁽⁷⁾ have analyzed constant temperature quasi-one dimensional flows. The former also assumed constant area, and constant magnetic field and included the Hall effect. The latter neglected the Hall effect, assumed constant electric field, and took the flow velocity proportional to a power of x . The percent ionization was also assumed small so the gas was assumed perfect. In order to illustrate the information available from these analysis, consider the illustrative example calculated by Kerrebrock. Assuming Helium seeded with

Cesium at 3000°K, an initial B_z of 10,000 gauss, and an initial M of unity, he calculated an $I_{sp} \cong 670$ seconds for an accelerator length of 10 centimeters. As will be seen shortly much higher specific impulses can be obtained at higher temperatures and percentages of seed material.

In the case of the accelerator proposed by Wood⁽⁶⁾ $E_x \neq 0$ and E_y varies with x, since B_z is assumed constant and no Hall currents are permitted to flow. Here, segmented electrodes are essential. In the other calculation⁽⁷⁾ it was assumed that $u \propto x^n$ so that the channel cross sectional area depends on the choice of n, being constant when $n = 0.25$. Regardless of the area variation for this second case the distance between electrodes must be constant since E_y is assumed constant and continuous electrodes are used.

An alternate approach to the problem of accelerating a plasma in a crossed field device without excessive increase of static temperature is to rapidly increase the flow area in the flow direction. This has the effect of converting the Joule heat into kinetic energy by the usual thermodynamic expansion process. Since the more rapid the channel expansion the less valid the quasi-one dimensional theory Podolsky⁽⁸⁾ and Sherman⁽⁹⁾ have postulated a source flow model of the accelerator. Such a model is shown in figure 13-1.

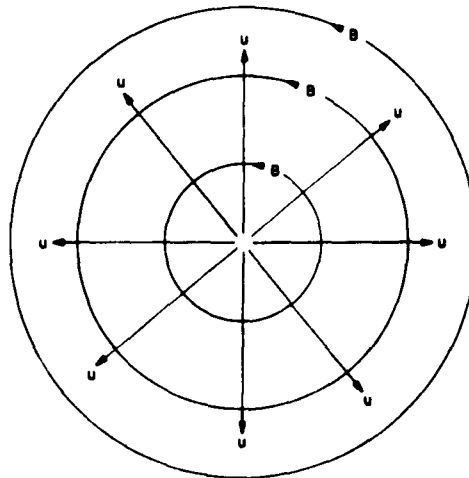


Figure 13-1. Source Flow Model of Crossed Field Accelerator

Here it is assumed that a radial flow occurs in the presence of an azimuthal B field which varies in magnitude as r^{-1} . The electrodes are plane surfaces perpendicular to the source axis. The accelerator then can have any divergence angle, θ , if it is assumed to be that portion of the source flow located between two radii. The geometry is shown in Figure 13-2.

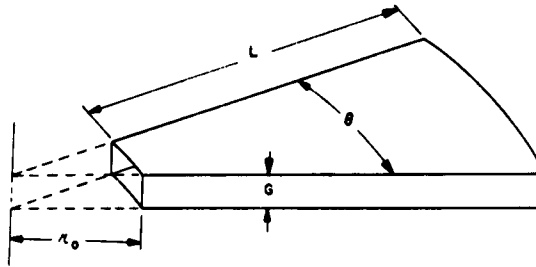


Figure 13-2. Accelerator Duct Geometry

The equations governing this flow are equations (8.1 - 8.8) written in cylindrical coordinates. For $\frac{\partial}{\partial \theta} = \frac{\partial}{\partial z} = 0$ the following system of equations are found.

Equation of Motion

$$\rho u \frac{du}{dr} = - \frac{dp}{dr} + \frac{\sigma' B_0 r_0}{r} \left(E_0 - \frac{ur_0 B_0}{r} \right) \quad (13.10)$$

Conservation of Energy

$$\rho u \frac{de}{dr} = - \frac{p}{r} \frac{d}{dr} (ru) + \left(\sigma' E_0 - \frac{ur_0 B_0}{r} \right)^2 \quad (13.11)$$

Mass Conservation

$$\rho u r = \rho_0 u_0 r_0 \quad (13.12)$$

where

$$\sigma' = \sigma / \left[1 + (\sigma \beta B)^2 \right] \quad \sigma \beta B \sim \omega \tau$$

and the subscript zero denotes conditions at the accelerator entrance.

The plasma can be assumed to be a perfect gas or, if desired, property variations can be included^(8,9). Also, one can assume the electrodes segmented and thereby neglect $\omega \tau$ ⁽⁸⁾, or they can be assumed solid so that $\omega \tau$ is calculated during the course of the solution and σ' used.⁽⁹⁾ In the former case, calculations have been made for pure Lithium vapor at low pressures ($P_1^0 \sim 1$ mm Hg), and it has been shown that I_{sp} values in the range 5-6000 seconds should be possible over reasonable accelerator lengths. For the latter analysis, in which solid electrodes were assumed, calculations have been carried out under the following conditions:

$$\begin{aligned} r_0 &= 1 \text{ cm} & M_0 &= 1.5 \\ B_0 &= 11,000 \text{ gauss} & K &= 1.5 \\ p^0 &= 0.233 \text{ atm} \\ T^0 &= 5000^\circ \text{K} \end{aligned}$$

for various mixtures of Lithium and Helium. Some typical results for pure Lithium are shown in Figure 13-3.

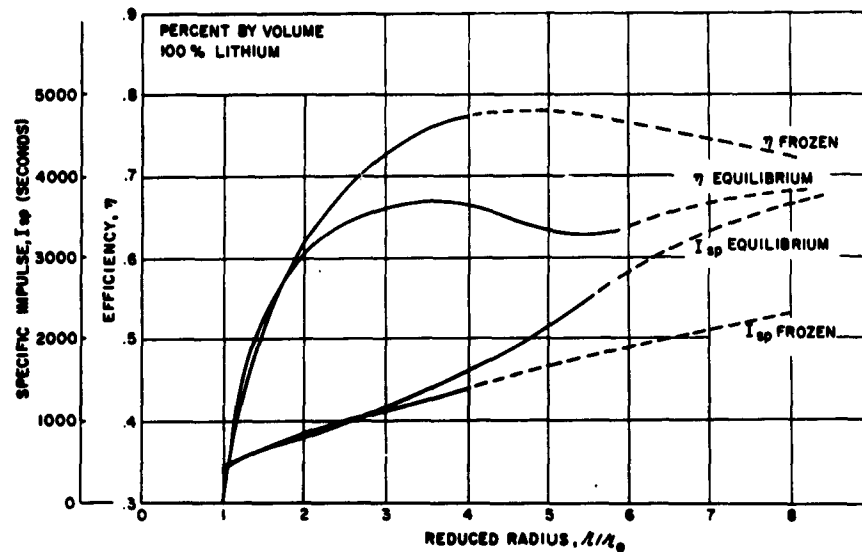


Figure 13-3. Crossed Field Accelerator Specific Impulse and Efficiency

It should be noted that provision was made in the calculation to assume that the flow was either in a shifting ionization equilibrium or the ionization was frozen. The essential feature shown in these calculations is that even for frozen flow an $I_{sp} \sim 2200$ seconds is possible along with an efficiency greater than 70%, and the accelerator is only 8 cm long. Even better performance would have been calculated had the electrodes been assumed segmented.

So far it has been shown both by the quasi-one dimensional analysis and the source flow model that higher specific impulses than are possible with plasma jets should be possible without excessive thermal, dissociation, or ionization losses. The question of thermal losses into the channel walls has not yet been considered, and will be taken up next.

In chapter 12 an analysis of a compressible magnetohydrodynamic boundary layer was described for which the free stream velocity varied as x^n . If the results of this analysis are applied to the crossed field accelerator some estimates of the heat loss to the wall can be made. In particular when $n = 0.25$ the following relation was derived for $M < 2.5$,

$$\frac{N_u}{\sqrt{R_e}} \approx 5 \quad (13.13)$$

where $P_R = 1$ was assumed and the Nusselt number was defined as

$$N_u \equiv - \frac{\dot{q}_\omega x}{K_\infty (T_\infty - T_\omega)} \quad (13.14)$$

where $()_\infty$ denotes some reference point in the free stream.

so that the lower the flow Reynolds number the lower the magnitude of the heat flux. Since such fluxes can be the order of magnitude of several KW/cm² the practical problem of finding a way to remove so much heat may make it necessary to reduce the flux by lowering the Reynolds number or the temperature difference $(T_\infty - T_\omega)$ or both. As far as the accelerator efficiency is concerned, however, it will be shown that high Reynolds numbers would be desirable. Define an efficiency as the ratio of the exhaust kinetic energy to the exhaust total enthalpy plus heat losses along the way. Then

$$\eta' = \frac{\frac{1}{2} \rho_e v_e^3 A_e}{\rho_e v_e A_e \left(\frac{1}{2} v_e^2 + c_p T_e \right) + \dot{q}_\omega L C} \quad (13.15)$$

If \dot{q}_ω is taken from equation (13.14) with N_u given by equation (13.13) the above expression for efficiency can be rewritten as

$$\eta' = \left[1 + \frac{2}{(\gamma-1) M_e^2} \left\{ 1 + \frac{60 (1 - \frac{T_\omega}{T_\infty}) \sqrt{\frac{v_o}{v_e}}}{R_e^{1/2}} \right\} \right]^{-1} \quad (13.16)$$

where the Reynolds number is based on the exit velocity and channel width and v_o is a reference velocity near the accelerator entrance. It was also assumed that the channel was square so that $A_e = \omega^2$, and C (the circumference) = 4ω . Since $q_\omega \propto \frac{1}{x}$ in equation (13.14) an average length was used = $\frac{L}{3}$. The variation of ρ along the channel was neglected and the reference length x_o was assumed equal to ω .

Qualitatively then, the accelerator efficiency will be maximized when M_e and R_e are as large as possible. It is also desirable to have $T_\omega \sim T_\infty$ and $v_e \gg v_o$, as one might have expected. Strictly speaking the above relation applies only to the special case considered by Kerrebrock (Chapter 12). None the less, the Mach number and Reynolds number dependencies should be valid for any crossed field accelerator of this type.

Before concluding the discussion of the theoretical aspects of the crossed field accelerator the results of some quantitative calculations of heat loss⁽¹⁰⁾ will

be described. Making use of the example just described with Argon seeded with Potassium and with $T_w = 1500^\circ\text{K}$ and $T_\infty = 3000^\circ\text{K}$, integration of the heat flux over the channel length leads to a heat loss of 3.26 kw per electrode. Then, in hopes of reducing the heat flux as well as the leaving thermal losses noted earlier, the possibility of operation in a non-equilibrium mode can be considered. In this case Joule heating in the low temperature layer near the wall is substantially reduced since the electron temperature can be quite high in this region. The principle heat flux then occurs by virtue of the electron flux in the presence of a temperature gradient. For the same case cited above the heat flux is calculated to be⁽¹⁰⁾

$$q_{\text{anode}} = 0.972 K_w \quad q_{\text{cathode}} = 0.065 K_w$$

where $(T_e)_\infty = 3500^\circ\text{K}$ and $T_\infty = 1746^\circ\text{K}$ while $T_w = 1500^\circ\text{K}$. As can be seen, the total heat flux is considerably reduced, and the asymmetry due to the direction of electron flux is apparent. Although the above analysis is certainly quite preliminary and involves many assumptions, the trend of the results seems to be in the correct direction. Finally, it should be noted that operating under non-equilibrium conditions should not reduce frozen flow losses but only thermal leaving losses, and perhaps heat flux.

Turning now to the experimental verification of the above developments only very preliminary results are presently available. It will be of interest, however, to review work currently in progress. Perhaps the first experimental crossed field accelerator was built by Carter and Wood⁽¹¹⁾. The device they have conceived is designed according to the constant T, E, and A analysis mentioned earlier, and so has segmented electrodes. A flow of 2.6 gm/sec of Nitrogen seeded with Cesium is heated to a total temperature of 6900°K before entering the 1 cm^2 channel at $M = 2$. With the use of a 12,000 gauss magnet preliminary experiments have demonstrated the feasibility of the concept but have not yielded any detailed measurements. More recently Hogan⁽¹²⁾ in a shock tube experiment demonstrated a two fold increase in specific impulse in a crossed field device. In this experiment a 1-1/2 inch diameter combustion driven shock tube heats pure Argon to 12000°K at one atmosphere while accelerating it to $M = 2$. Under these conditions $\sigma \sim 4500$ mhos/meter and the interaction parameter Q is sufficiently large to create a sizeable influence on the flow. Starting with an $I_{sp} \sim 500$ sec Hogan measures an $I_{sp} \sim 1000$ sec after acceleration by the use of a magnetic field of 1500 gauss. He also estimates $\eta \cong 50\%$. Although these results are encouraging the specific impulse is still too low. Since these experiments were

run at relatively high pressures ωT was small enough to be neglected and electron heating did not occur.

Most recently some continuous experiments have been carried out by Demetriades⁽¹³⁾ in which a crossed field accelerator was operated on unseeded Argon but at lower pressures and temperatures than used by Hogan. In this case the Hall effect must be considered and non-equilibrium ionization of the plasma is a real possibility. A diagram of the experimental apparatus is shown in Figure 13-4.

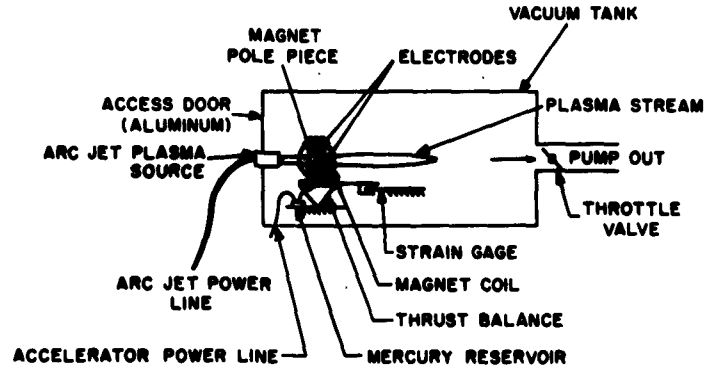


Figure 13-4. Experimental Apparatus for Crossed Field Accelerator Experiments

In this arrangement the arc jet exhausts into the vacuum tank and the crossed field accelerator acts on the jet itself. The entire accelerator assembly is balanced on a thrust stand and thrust is measured directly by means of strain gauges. Some typical experimental data are reproduced in Figure 13-5.

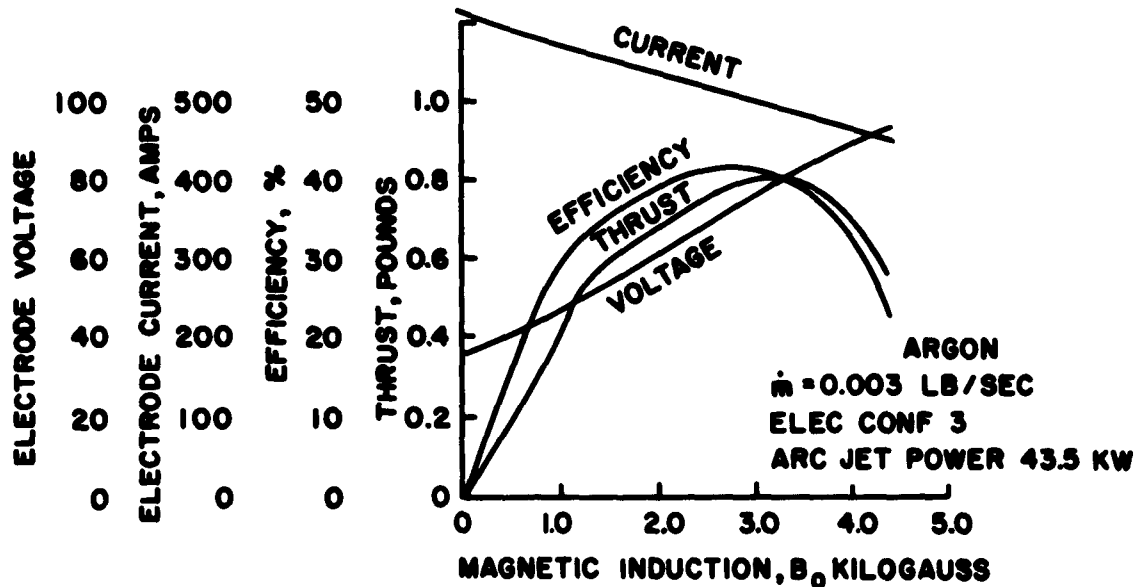


Figure 13-5. Typical Performance of a Crossed Field Accelerator

The drop off in thrust with B can be generally attributed to the Hall reduction in cross wise current occuring when solid electrodes are used and $\omega\tau > 1$. For the above data a maximum specific impulse of 660 seconds (counting the 400 seconds available initially from the arc jet) is obtained at an efficiency of 42%. Specific impulses as high as 1400 seconds have also been reported, presumably at similarly high efficiencies. Complete data on this device which demonstrates $I_{sp} \cong 2000$ sec at high efficiencies is not available as yet.

In summary, then, theoretical calculations indicate that the crossed field accelerator should operate in the I_{sp} range over 1500 seconds with reasonable efficiencies. It is unlikely that efficient operation will be possible for $I_{sp} \cong 4000$ seconds. To date experimental verification has been achieved of the basic feasibility of such devices, but detailed demonstration of both high I_{sp} and η for long periods of time has not yet been accomplished.

13.3 THE HALL CURRENT ACCELERATOR

As was shown in the preceeding section there is a general desire to increase the magnetic field and lower the density in order to create larger values of Q, the interaction parameter. This, of course, raises $\omega\tau$ to quite high values and the question must be raised as to whether or not there may be other accelerator geometries more suitable to high $\omega\tau$ operation. Two configurations which have been suggested, and which we will call Hall current accelerators, will be discussed here.

Both devices, in their two dimensional configuration, use segmented electrodes in this case to encourage the flow of Hall currents rather than surpress them. In these devices it is the Lorentz force due to the Hall currents that does the accelerating. The first device is shown in Figure 13-6.⁽⁵⁾

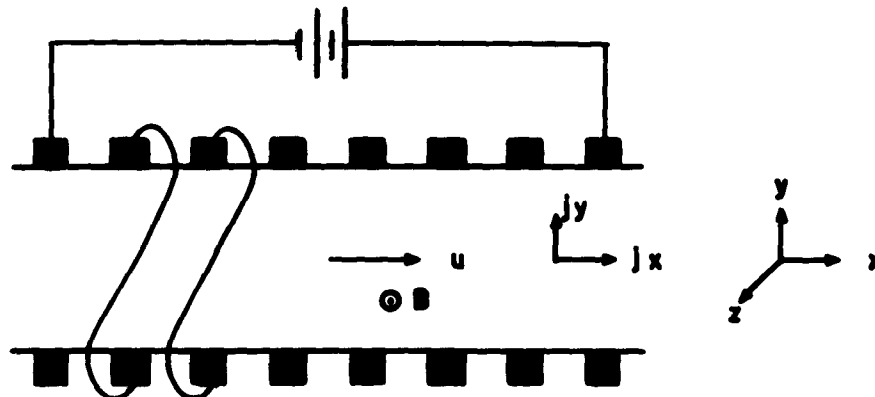


Figure 13-6. Hall Current Accelerator I

Here a voltage is applied between electrodes at the channel inlet and outlet. The resulting current flow interacting with the transverse B field induces a Hall current to flow across the channel. Short circuiting each pair of opposing electrodes allows this current flow unimpeded. Interaction between this Hall current and the applied B field yields the accelerating force.

An alternate geometric arrangement is shown in Figure 13-7. (5,14)

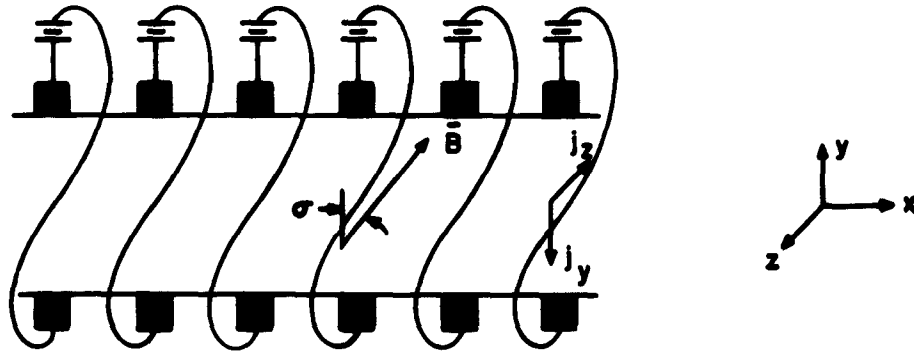


Figure 13-7. Hall Current Accelerator II

In this device now an oblique magnetic field is applied. An applied electric field then causes a current to flow which interacts with the x component of the applied magnetic field to create a transverse Hall current flow, j_z . This current interacting with the y component of the magnetic field yields the accelerating force.

Each of the above devices is also feasible in a coaxial or annular geometry. For accelerator I one would have an annular space with a radial magnetic field. Applying a longitudinal electric field would now cause an azimuthal Hall current which would, as before, interact with the radial magnetic field to yield the accelerating force. In the case of accelerator II the inner and outer walls of the annulus would be composed of concentric rings between which an applied electric field would be applied. In fact this geometry is generated if the channel of Figure 13-7 is rotated about an axis parallel to the flow and below the channel. The mode of operation is precisely as before. The advantage of the annular geometry lies principally with accelerator I where by this device the multitude of short circuited electrodes is avoided.

For simplicity, a brief analysis of each of the above accelerators will be given, when the flow velocity is assumed to be uniform, for the two dimensional configurations (small cross flows will be neglected). Expanding the Generalized

Ohms Law (equation (8.8)) into its three components yields

$$j_x = \sigma_o \left[E_x + v B_z - \omega B_y - \beta (j_y B_z - j_z B_y) \right] \quad (13.17)$$

$$j_y = \sigma_o \left[E_y + \omega B_x - u B_z - \beta (j_z B_x - j_x B_z) \right] \quad (13.18)$$

$$j_z = \sigma_o \left[E_z + u B_y - v B_x - \beta (j_x B_y - j_y B_x) \right] \quad (13.19)$$

For accelerator I, however, $j_z = B_x = B_y = E_z = v = \omega = 0$. Thus

$$j_x = \frac{\sigma_o}{1 + (\omega\tau)^2} \left[E_x - \omega\tau (E_y - u B_z) \right] \quad (13.20)$$

$$j_y = \frac{\sigma_o}{1 + (\omega\tau)^2} \left[E_y - u B_z + \omega\tau E_x \right] \quad (13.21)$$

Or defining $E_x = K \omega\tau u B_z$ these become

$$j_x = \frac{\sigma_o u B_z (\omega\tau)}{1 + (\omega\tau)^2} \left[1 + K \right] \quad (13.22)$$

$$j_y = \frac{\sigma_o u B_z}{1 + (\omega\tau)^2} \left[(\omega\tau)^2 K - 1 \right] \quad (13.23)$$

Then the Lorentz force, $\vec{J} \times \vec{B}$ is simply

$$F_x = \frac{\sigma_o u B_z^2}{1 + (\omega\tau)^2} \left[(\omega\tau)^2 K - 1 \right] \quad (13.24)$$

Clearly one must have $K > \frac{1}{(\omega\tau)^2}$ in order for this device to operate as an accelerator. However, one cannot set K too large or the efficiency will fall. To illustrate this the value of K at which η is a maximum will be calculated.

Define η as

$$\eta = \frac{F_x u}{E_x j_x} = \frac{(\omega\tau)^2 K - 1}{(\omega\tau)^2 K (1 + K)} \quad (13.25)$$

Differentiating and setting equal to zero yields

$$K_{opt.} = \frac{1 + \sqrt{1 + (\omega\tau)^2}}{(\omega\tau)^2} \quad (13.26)$$

When $\omega\tau$ becomes very large $K_{opt.} \rightarrow (\omega\tau)^{-1}$ and $\eta \rightarrow (1 + \frac{2}{\omega\tau})^{-1}$. Also

the axial force $F_x \rightarrow \frac{\sigma_0 u B_z^2}{\omega\tau}$. If desired this can be compared to the axial force in a crossed field device with high $\omega\tau$ and segmented electrodes. For this case $F_{x1} = \sigma u B^2 (K_1 - 1)$ where now $K_1 \equiv E_y/uB$ and the efficiency is $\eta = K_1^{-1}$. For the same efficiency in each accelerator we find $F_{x1} = \frac{2\sigma u B^2}{\omega\tau}$

which is double the value for the Hall accelerator. At first glance it would seem that the crossed field device is twice as effective as the Hall accelerator I. That this is not necessarily true can be seen by considering equations (13.24) and (13.25) again. As shown in Figure 13-8 the efficiency does not drop off very rapidly at all for $K > K_{opt.}$ Thus, let us consider an example for which $\omega\tau = 10$, and $K = 0.2$. In this case $\eta \cong 79\%$ as contrasted to 83% when $K = 0.1$. However now $F_x = 0.19 \sigma_0 u B_z^2$. For the crossed field accelerator with $\eta = 79\%$ the axial force is now $F_{x1} = 0.26 \sigma_0 u B_z^2$, so that apparent disadvantage is greatly reduced.

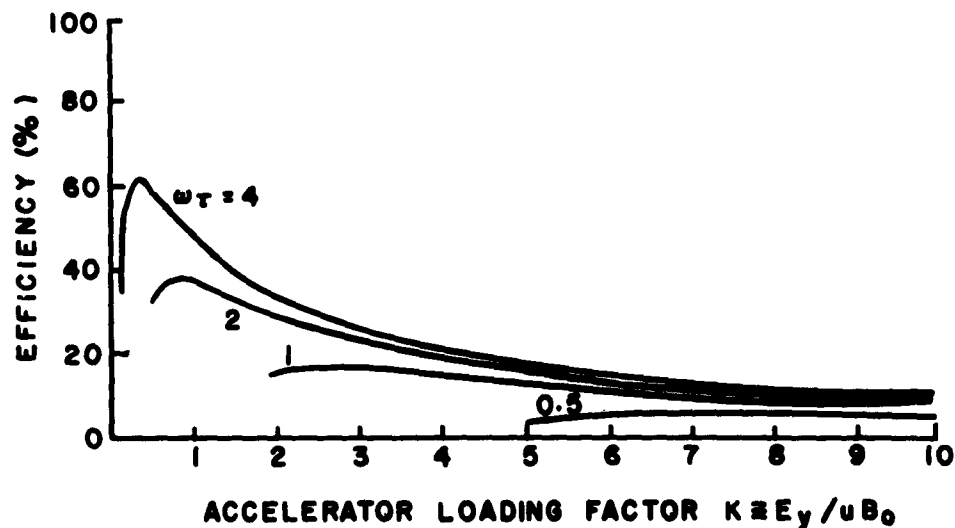


Figure 13-8. Hall Accelerator I Efficiency Versus Loading Factor

In general then the Hall accelerator I will be comparable in performance to the crossed field device at large $\omega\tau$ values. Despite this and the fact that a single power supply may be used this device has been relatively little explored to date.

Consideration will now be given to the second type of Hall accelerator illustrated in Figure 13-7. For this case it will be assumed that $j_x = B_z = E_z = v = \omega = 0$, so that the current relations yield

$$j_y = \frac{-\sigma u B \cos \alpha (K_2 + (\omega\tau)^2 \sin^2 \alpha)}{(1 + (\omega\tau)^2 \sin^2 \alpha) (\omega\tau \sin \alpha)} \quad (13.27)$$

$$j_z = \frac{-\sigma u B \cos \alpha (K_2 - 1)}{(1 + (\omega\tau)^2 \sin^2 \alpha)} \quad (13.28)$$

where

$$K_2 = \frac{-\omega\tau E_y \sin \alpha}{u B \cos \alpha}$$

and B denotes the magnitude of \underline{B} . The axial propulsive force is $F_x = -j_z B_y = -j_z B \cos \alpha$ so that we must require $K_2 > 1$ in order for the device to function as an accelerator.

Without going into any more detailed analysis some of the operating characteristics of this device can be deduced. First, if $\alpha = 0$ nothing occurs other than Joule heating of the plasma since $\underline{j} \times \underline{B} = 0$. Alternately, when $\alpha = 90^\circ$ both an azimuthal and a radial current will flow again resulting in Joule heating. If the coaxial geometry is employed a rotational flow will be induced, and if $\omega\tau \gg 1$ most of the energy will appear as rotational kinetic energy. This rotational kinetic energy can, perhaps, be converted into directed kinetic energy.

When $j_x = 0$ as has been assumed the efficiency of the above device can be shown to be comparable to the crossed field device⁽¹⁴⁾. If, however, segmented electrodes are not used $E_x = 0$ and the devices performance will be quite poor.⁽⁵⁾

13.4 PULSED ACCELERATORS EMPLOYING ELECTRODES

For the remainder of this chapter the discussion will be devoted to accelerators which operate in an unsteady fashion. Generally speaking the basic advantage of an unsteady device is that a plasma of very high energy or temperature can be created and handled without any severe wall erosion problem

so that efficiencies can be kept high. In other words, the thermal lag of the accelerator and the short time of plasma contact with it combine to keep the material surface temperatures low.

Attention will be devoted in the present section to those pulsed accelerators which use electrodes to bring current into and out of the plasma. The related device which operates inductively without electrodes will be treated next.

The basic mode of operation of the pulsed accelerator with electrodes is best illustrated by the sketch shown in Figure 13-9.

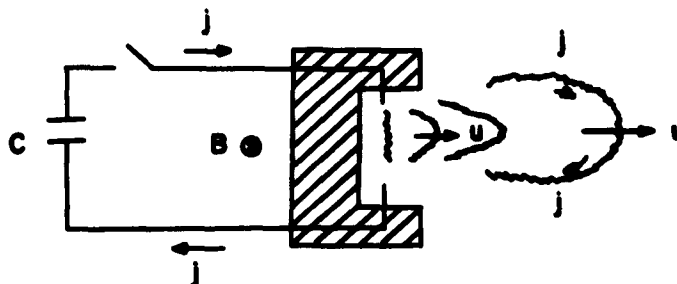


Figure 13-9. Schematic of a Pulsed Accelerator with Electrodes

When the switch is closed a very high voltage is applied to the gas between the electrodes. An arc then forms creating a plasma and discharging the capacitor. As the current flows a strong magnetic field, B , is generated, and the plasma is blown away from the electrodes by the Lorentz force due to the current in the arc. With sufficiently large current flows the plasma ejected can reach very high velocities.

Since the plasma in a device such as this is essentially unconfined much of the energy imparted to it appears as radial motion. In addition, the Lorentz force is only applied for a very short time since the arc column quickly grows in length and detaches from the electrodes. For these two reasons the efficiency of the simple device is quite poor.

One approach taken to improve the efficiency of such a device was to confine the arc within a T-tube geometry⁽¹⁵⁾ such as shown in Figure 13-10a. Also, in order to get the largest Lorentz force the current return lead from the capacitor was passed close to the region of the initial discharge. Although originally conceived as a device to generate high velocities alone it has achieved efficiencies in the 5-10% range when operated as a propulsion device⁽¹⁶⁾.

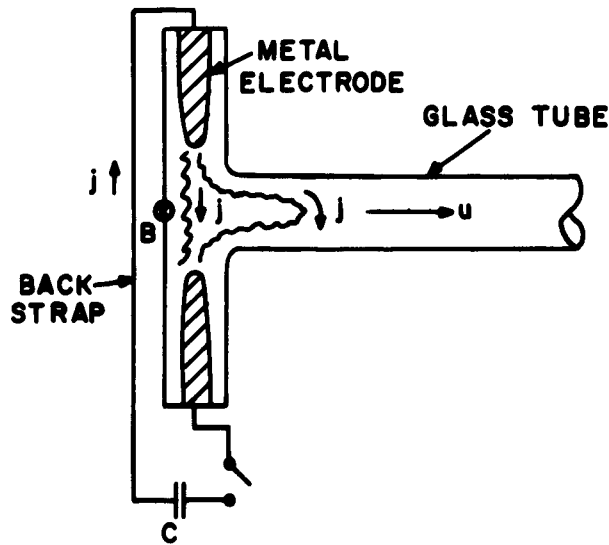


Figure 13-10a. T-Tube Plasma Accelerator

An alternate approach to a higher efficiency device is the rail accelerator shown in Figure 13-10b.

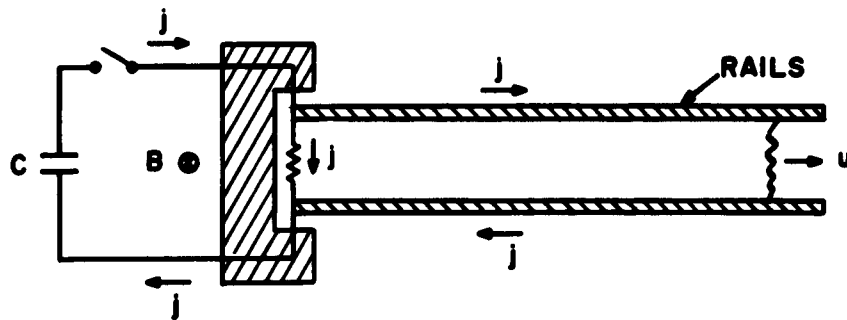


Figure 13-10b. Rail Plasma Accelerator

Here rails help carry the current to the arc as it accelerates, so that the propulsive force acts on the plasma for a longer time. Despite this, experiments with such devices have yielded very low efficiencies since the plasma is still relatively unconfined.

A logical combination of the above two approaches should, however, yield an efficient device. Such in fact has been found to be the case. The first device combining both of these features, rails and confinement, was built by Marshall⁽¹⁷⁾.

Basically, this device consists of a pair of concentric rails whereby the confinement is accomplished between the two cylindrical electrodes. Schematically it is shown in Figure 13-11. Experiments carried out on this and related devices have shown that specific impulses in the range of 5000-25,000 seconds are possible with efficiencies on the order of 50%. Compared to earlier devices with efficiencies of 1% the coaxial device apparently successfully increases the coupling of the capacitor energy to the plasma and prevents the increase in arc resistance as the plasma accelerates. In addition to the increased efficiencies it has also been reported that little or no electrode ablation has been observed so that long life operation may be possible.

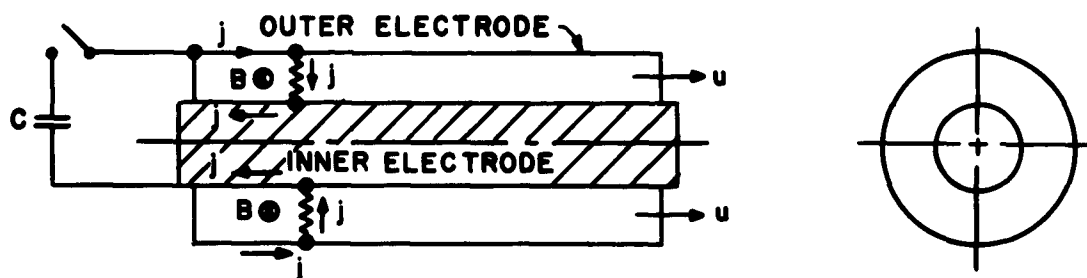


Figure 13-11. Marshall Coaxial Plasma Gun

Before proceeding to the discussion of the continuous (rapid pulsing) operation of such plasma accelerators it would be of interest to note some of the numerous geometric arrangements analagous to the device shown in Figure 13-11. Most obvious is the simple two dimensional rail system contained within a appropriate channel structure. Similar favorable I_{sp} and η values have been obtained recently with such a device⁽¹⁸⁾. Other devices with essentially the same coaxial geometry as the Marshall device have been operated by Avco⁽¹⁹⁾ and General Electric⁽²⁰⁾. Finally, a novel geometric arrangement has been proposed by Republic Aviation⁽²¹⁾ and is shown in Figure 13-12

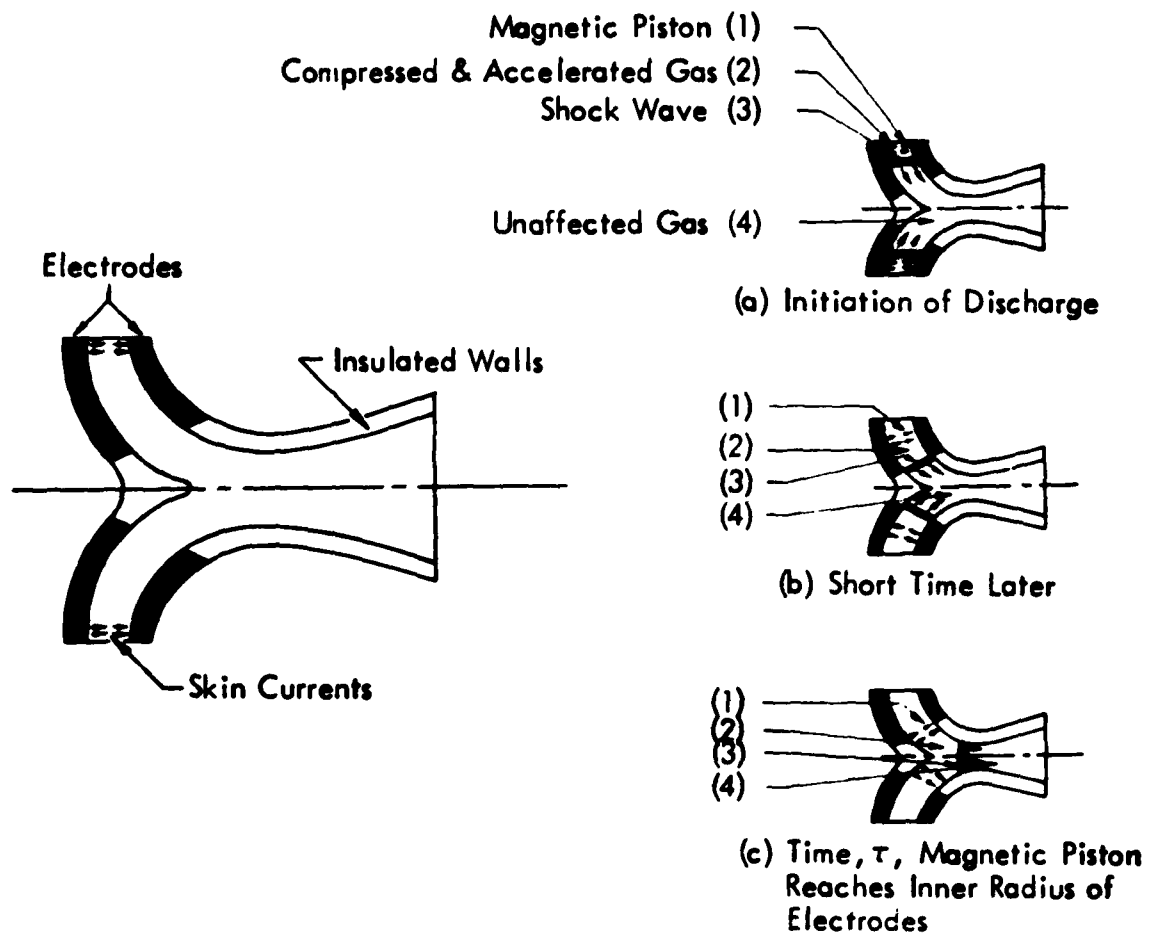


Figure 13-12. Pulsed Pinch Plasma Accelerator

If this device were two dimensional it would be, essentially, a shaped rail system followed by an aerodynamic nozzle. In this way reasonably good confinement is obtained and, in addition, some of the plasma thermal energy can be converted to axial kinetic energy by the nozzle.

So far no distinction has been drawn between the mode of operation in which the gas is admitted in a pulse and the high voltage breaks it down and the mode in which the gas flows in continuously and is broken down by a pulsed electric field. The distinction is essential, however, if the pulsed electrodeless accelerator is to be used for continuous operation as a space propulsion device. In general the weight of the capacitors needed for a given size engine will be minimized if a high pulsing rate is possible. This is due to the fact that the stored energy per pulse required is less the more pulses per second, and the greater the stored energy the heavier the capacitor. Now, when the gas flow is continuous a high power fast acting switch is needed, and there is some question as to whether such a switch would be reliable over extended periods of time. An alternate approach would be to pulse the gas in and maintain a constant applied voltage. The problem that arises here is that the low pressure gas at the front of the gas pulse tends to break down first and the magnetohydrodynamic interaction is poor. One of perhaps several solutions is to use a two stage device⁽²²⁾. Here a low power switch triggers a small T-tube which then discharges into a larger coaxial accelerator across which is placed the main power supply. The partially ionized plasma entering the second stage has a sharp pressure front so that the breakdown is favorable to good accelerating action. Using this device a life test of 60 hours with a pulsing rate of 1000/minute was achieved. For this particular test a thrust of 0.02 lbs., an I_{sp} of 9000 seconds, and an η of 52% were reported⁽²²⁾.

Clearly then, the pulsed magnetohydrodynamic accelerator employing electrodes seems capable of long time operation at high specific impulses and efficiency. It is yet to be demonstrated that they can operate well in the 2000-4000 second range also. If this can be shown, however, they may provide the interesting possibility of a single engine capable of operation over a wide range of I_{sp} .

13.5 ELECTRODELESS ACCELERATORS

In this final section the type of pulsed accelerator which operates inductively will be discussed. The principle of operation can be readily illustrated in terms of the single pulse mode of operation. Consider a tube filled with ionized gas,

open at one end, and with a single turn coil around the closed end as shown in Figure 13-13.

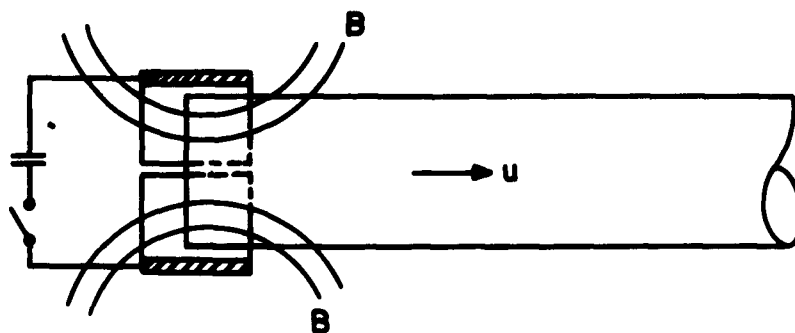


Figure 13-13. Single Pulse Electrodeless Accelerator

When the switch is closed, discharging the capacitor, a rapidly time varying magnetic field is generated. This, in turn, creates an azimuthal electric field, and since the plasma is a conductor an azimuthal current flows. The interaction of this induced current and the radial component of the magnetic field present results in a Lorentz force in the axial direction. In the event that the plasma is a poor conductor the fraction of energy input which goes into work by the Lorentz force will be small compared to energy input into Joule heating of the coil. One measure of the efficiency capability of such a device will then be the Magnetic Reynolds number, since in general this parameter describes the coupling between the applied magnetic field and the induced current.

So far nothing has been said concerning the method for initially ionizing the plasma. Most investigators have actually started with initially cool gas and used the single turn coil to breakdown the gas as well as provide the accelerating action just described. This technique of ionizing a gas is an old one known as the "ring discharge". In simplest terms, the azimuthal electric field is made strong enough to create a discharge in the gas. Since this field is at a maximum near the wall the discharge initiates there and the resulting current sheet is driven inward towards the tube axis⁽²³⁾. As can be seen, when the ring discharge is used to establish the conductivity the acceleration process is extremely complicated, and because of this, principally experimental analysis have been carried out.

One of the more extensive studies has been carried out by Miller⁽²³⁾ whose measurements can be interpreted in terms of specific impulse and efficiency.

Measurements of I_{sp} up to ~ 1700 seconds were made. The measured overall efficiencies were on the order of 1-2%, and can be explained as follows. It was found that of the initial stored energy in the capacitors only 1/3 reached the field. Of this amount only 5-10% was successfully transferred to the plasma. Finally, the total energy of the plasma stream was apparently evenly split between thermal and kinetic energies. Clearly poor coupling between the magnetic field and the plasma accounts for a major energy loss. Actually there is no reason to assume that using a ring discharge in this device would be more efficient than preionizing and then activating the coil. In fact, it would seem that preionizing the plasma such that σ is high initially should lead to a more efficient coupling. Carrying this concept further experiments have been conducted in which the preionization is provided by an RF coil and the single drive coil is operated with 10 KC alternating current⁽²⁴⁾. With the drive coil operating this way the accelerator operated in a quasi-steady fashion and some plasma acceleration was measured.

In addition to the possibility of operating the single coil on AC one can also build an accelerator tube with a number of coils. If the coils are then fired in succession with the proper timing the plasma pulse should receive several accelerations before being ejected. In this way it may be possible to achieve higher specific impulses at a corresponding higher efficiency.

A logical extension of this idea would be to operate each coil on AC, again with the proper timing. This then brings us to the consideration of the traveling wave concept of electrodeless accelerator. A number of investigators have studied the traveling wave accelerator from several points of view. Basically, they are all manifestations of the simple arrangement shown in Figure 13-14.

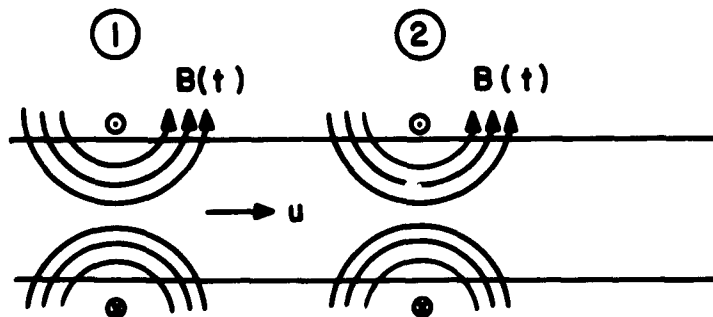


Figure 13-14. Traveling Wave Accelerator

The mode of operation is as follows: At $t = 0$ a step function of voltage is applied and a current pulse begins to travel down the helical transmission coil. When it reaches position (1) it accelerates plasma in the downstream direction. As the plasma reaches position (2) the first current pulse arrives there and gives it a second push. At about this time another current pulse arrives at position (1) again, and the process is repeated. Preliminary experiments with a device similar to that described have demonstrated that an interaction can be achieved but efficiency and specific impulse are still low⁽²⁵⁾; $I_{sp} \cong 1000$ sec, $\eta \cong 1\%$. If the coils are spaced more closely than shown in Figure 13-14 and the plasma pressure is low enough so that it is collisionless one has, effectively, a series of magnetic bottles such as shown in Figure 13-15.

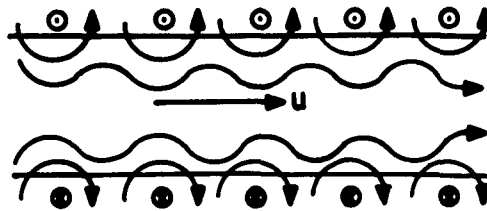
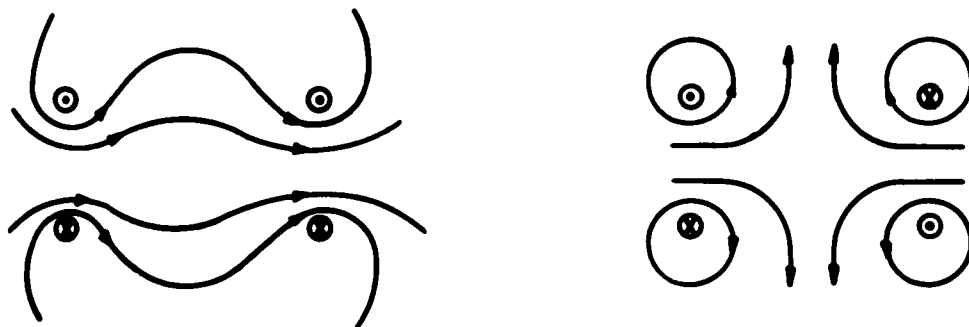


Figure 13-15. Traveling Wave Accelerator with Magnetic Confinement

Such a device is still only in the conceptual stage⁽¹⁹⁾.

It should also be noted that if the current is reversed in every other coil then one can create what is essentially a traveling wave machine which behaves as if a series of cusps rather than magnetic mirrors were traveling in the flow direction.



(a) BOTTLE

(b) CUSP

Figure 13-16. Comparison of Magnetic Bottle and Cusp Field Configurations.

The cusp geometry has been proposed for Thermonuclear fusion work in which the stability of confinement is the essential problem. Whether or not a similar approach is necessary or desirable for a space propulsion device is not as yet clear.

As noted earlier the successful operation of all such devices will depend on effective coupling between the applied magnetic field and the plasma. The ideal situation would involve zero slip between the magnetic field lines and the plasma. In other words, one would want $R_m \rightarrow \infty$. Practically speaking such a condition will be difficult to obtain in a basically low temperature and low conductivity plasma. For solid copper wires with their very high electrical conductivity it is well known that such a condition can be met and that induction motors are indeed a practical reality.

REFERENCES

1. Corliss, W.R. Propulsion Systems for Space Flight, McGraw-Hill Book Co., New York, 1960.
2. Camac, M. "Plasma Propulsion of Spacecraft", *Astronautics* Vol. 4, October 1959
3. Demetriades, S.T. "Plasma Propulsion - Part I", *Astronautics* Vol. 7, March 1962
4. Gourdine, M.C. "Recent Advances in Magnetohydrodynamic Propulsion" *ARS Journ.* 31, 1670 (1961)
5. Sutton, G.W. and Gloersen, P. "Magnetohydrodynamic Power and Propulsion" published in *Magnetohydrodynamics. Proceedings of the Fourth Biennial Gas Dynamics Symposium*, edited by A.B. Cambel, T.P. Anderson, M.M. Slawsky, Northwestern University Press, 1961.
6. Wood, G.P., Carter, A.F., Lintz, H.K. and Pennington, J.B. A Theoretical Treatment of the Steady Flow, linear, crossed field, direct current plasma accelerator for inviscid, adiabatic, isothermal, constant area flow NASA TR R-114, 1961.
7. Kerrebrock, J. and Marble, F.E. Constant Temperature Magnetogasdynamic Channel Flow. *J. Aerospace Sci.* Jan. 1960.
8. Podolsky, B. and Borman, G. Plasma Acceleration (S.W. Kash, ed.) Stanford University Press, Stanford, California, 1960.
9. Sherman, A. Theoretical Performance of a Crossed Field MHD Accelerator. *ARS Journal* 32, 414 (1962).
10. Oates, G.C., Richmond, J.K., Aoki, Y., and Grohs, G. Loss Mechanisms of a Low Temperature Plasma Accelerator. *ibid* ref. 5.
11. Wood, G.P., Carter, A.F., Sabol, A.P., and Weinstien, R.H. Experiments in Steady State Crossed Field Acceleration of Plasmas. *Phys. Fluids* 4, 652 (1961)
12. Hogan, W.T. Experiments with a Transient D.C. Crossed Field Accelerator at High Power Levels. 3rd Annual Engineering Aspects of MHD Symposium, Rochester Univ. 1962.
13. Demetriades, S.T. and Ziemer, R.W. Energy Transfer to Plasmas by Continuous Lorentz Forces. *ibid* ref. 5.
14. Sevier, J.R., Hess, R.V., and Brockman Brockman, P. Coaxial Hall Current Accelerator Operation at Forces and Efficiencies Comparable to Conventional Crossed Field Accelerators. *ARS Journal* 32, 78 (1962)

15. Kolb, A.C. Production of High Energy Plasmas by Magnetically Driven Shock Waves, Phys. Rev. 107, 345 (1957).
16. Harned, B.W. Magnetic Effect in a T-Tube, ARS Journal 30, 656 (1960).
17. Marshall, J., Jr. Performance of a Hydromagnetic Plasma Gun, Phys. Fluids 3, 134 (1960).
18. Maes, M.E. Experimental Investigation of the Confined Parallel Rail Pulsed Plasma Accelerator. *ibid* ref. 12.
19. Janes, G.S. Magneto hydrodynamic Propulsion, Avco Everett Research Laboratory, Research Report 90, August 1960.
20. Gloersen, P.,
Gorowitz, B., and
Palm, W. Experimental Performance of a Pulsed Gas Entry Coaxial Plasma Accelerator. ARS Journal, 31, 1158 (1961).
21. Granet, I. and
Guman, W.J. "Experimental Program for Plasma Pinch Space Engine". Journ. Amer. Soc. Naval Eng'rs. 73, 745 (1961).
22. Gloersen, P.,
Gorowitz, B.,
Hovis, W.A. Jr.,
and Thomas, R.B.,
Jr. An Investigation of the Properties of a Repetively Fired Two-Stage Coaxial Plasma Engine. *ibid* ref. 12.
23. Miller, D.B. Measurements on an Experimental Induction Plasma Accelerator. ARS Journ. 32, 549 (1962)
24. Barger, R.L.,
Brooks, J.D., and
Beasley, W.D. The Design and Operation of a Continuous Flow Electrodeless Plasma Accelerator NASA TN D-1004 Feb. 1962.
25. Jones, R.E. and
Palmer, R.W. Traveling Wave Plasma Engine Program at NASA, *ibid* ref. 12.

SPACE SCIENCES LABORATORY
MISSILE AND SPACE DIVISION

TECHNICAL INFORMATION SERIES

AUTHOR A. Sherman	SUBJECT CLASSIFICATION Magnetohydrodynamics	NO. R63SD5
TITLE MAGNETOHYDRODYNAMIC PROPULSION		DATE Jan. 7, 1963
REPRODUCIBLE COPY FILED AT MSD LIBRARY, DOCUMENTS LIBRARY UNIT, VALLEY FORGE SPACE TECHNOLOGY CENTER, KING OF PENNSA, PA.		G. I. CLASS I
		GOV. CLASS None
		NO. PAGES 30
<p>SUMMARY</p> <p>Within the present report the entire area of magnetohydrodynamic propulsion is reviewed. To begin with continuous flow plasma accelerators are discussed, and the current status of theoretical and experimental studies presented. Both the normal crossed field devices and the so-called Hall accelerators are described. It is shown that these devices offer the promise of efficient operation in the 2-4000 sec specific impulse range. Next the pulsed plasma accelerator with electrodes is considered. Experimental results with confined rail type devices are shown to yield high efficiencies for specific impulses greater than 5000 seconds for times of operation on the order of days. Similar results at lower specific impulses are not yet available. Finally, the experimental work on the pulsed electrodeless device is described, and it is shown that as yet relatively low efficiencies have been obtained. Some of the causes of such low efficiencies are discussed. The extension of this concept to the traveling wave machine is also included. It is intended that the present material will be one chapter of a forthcoming book.</p>		

By cutting out this rectangle and folding on the center line, the above information can be fitted into a standard card file.

AUTHOR Arthur Sherman

COUNTERSIGNED W. Fulton Joseph Fahr